3-M syndrome: a growth disorder associated with *IGF2* silencing

P G Murray[1,4], D Hanson[1], T Coulson[1], A Stevens[1], A Whatmore[1], R L Poole[2], D J Mackay[2], G C M Black[3,5] and **P E Clayton[1,4]**

[1]Centre for Paediatrics and Child Health, Institute of Human Development, Faculty of Medical and Human Sciences, University of Manchester, UK
[2]Faculty of Medicine, University of Southampton, Southampton, UK
[3]Centre for Genetic Medicine, Institute of Human Development, Faculty of Medical and Human Sciences, University of Manchester, UK
[4]5th Floor Research, Royal Manchester Children's Hospital, Central Manchester University Hospitals NHS Foundation Trust, Manchester Academic Health Sciences Centre, Oxford Road, Manchester M13 9WL, UK
[5]Genetic Medicine, St Mary's Hospital, Central Manchester University Hospitals NHS Foundation Trust, Manchester Academic Health Sciences Centre, Oxford Road, Manchester M13 9WL, UK

Correspondence should be addressed to P E Clayton
Email
peter.clayton@manchester.ac.uk

Abstract

3-M syndrome is an autosomal recessive disorder characterised by pre- and post-natal growth restriction, facial dysmorphism, normal intelligence and radiological features (slender long bones and tall vertebral bodies). It is known to be caused by mutations in the genes encoding cullin 7, obscurin-like 1 and coiled-coil domain containing 8. The mechanisms through which mutations in these genes impair growth are unclear. The aim of this study was to identify novel pathways involved in the growth impairment in 3-M syndrome. RNA was extracted from fibroblast cell lines derived from four 3-M syndrome patients and three control subjects, hybridised to Affymetrix HU 133 plus 2.0 arrays with quantitative real-time PCR used to confirm changes found on microarray. IGF-II protein levels in conditioned cell culture media were measured by ELISA. Of the top 10 downregulated probesets, three represented *IGF2* while *H19* was identified as the 23rd most upregulated probeset. QRT-PCR confirmed upregulation of *H19* ($P<0.001$) and downregulation of *IGF2* ($P<0.001$). Levels of IGF-II secreted into conditioned cell culture medium were higher for control fibroblasts than those for 3-M fibroblasts (10.2 ± 2.9 vs 0.6 ± 0.9 ng/ml, $P<0.01$). 3-M syndrome is associated with a gene expression profile of reduced *IGF2* expression and increased *H19* expression similar to that found in Silver–Russell syndrome. Loss of autocrine IGF-II in the growth plate may be associated with the short stature seen in children with 3-M syndrome.

Key Words
- SGA
- IGF2
- 3-M syndrome
- CUL7
- OBSL1
- CCDC8

Endocrine Connections (2013) **2**, 225–235

Introduction

3-M syndrome (named after the first three authors to describe the condition) is an autosomal recessive disorder characterised by impaired pre- and post-natal growth, facial dysmorphism (triangular shaped face, anteverted nares, full fleshy lips), prominent heels, normal intelligence and, in some, radiological features (slender long bones and tall vertebral bodies). It is caused by loss of function mutations in the genes encoding cullin 7 (*CUL7*) (1), obscurin-like 1 (*OBSL1*) (2) and coiled-coil domain containing 8 (*CCDC8*) (3). CUL7 is a scaffold protein forming part of an E3 ubiquitin ligase enzyme responsible for cytoplasmic protein degradation (4), while OBSL1 is a cytoskeletal adaptor protein which localises to the perinuclear region (5). The function of CCDC8 is unknown, but it binds to OBSL1 (3) and is required for p53-mediated apoptosis (6).

http://www.endocrineconnections.org
DOI: 10.1530/EC-13-0065

The mechanisms leading to the growth impairment seen in 3-M syndrome remain unclear, but are likely to relate to abnormalities in basic cellular growth as well as alterations in cellular responses to growth factor stimulation. The *Cul7*$^{-/-}$ mouse displays impaired pre-natal growth and abnormalities in placental vasculature, but dies from respiratory distress after birth (7). Suggested targets for the CUL7 containing E3 ubiquitin ligase enzyme include cyclin D1 (8) and IRS1 (9). Altered IGF-I signalling with increased activation of the downstream signalling molecule AKT was identified in *Cul7*$^{-/-}$ mouse embryonic fibroblasts (MEFs) (9), associated with poor cell growth and senescence. Overexpression of CUL7 in an immortalised cancer cell line leads to decreased p53-mediated apoptosis (10, 11, 12). In contrast to the data in MEFs, AKT signalling was reduced in human skin fibroblast cell lines derived from 3-M syndrome patients (13) (including one patient with a *CUL7* nonsense mutation). Alterations in the levels of the insulin-like growth factor-binding proteins (IGFBPs) have been identified in 3-M syndrome patient cell lines, both at the RNA level for IGFBP2 and 5 (14) and at the protein level for IGFBP2, 5 and 7 (13). Alterations in IGFBP levels and IGF-I signal transduction are seen in cell lines with *OBSL1* and *CCDC8* mutations (13) as well as *CUL7* mutations; there is, however, a paucity of other data on the link between *OBSL1*, *CCDC8* and *CUL7* and the mechanism of growth impairment.

Although 3-M syndrome is considered to be a relatively uncommon disorder, it is probably an under recognised condition (6); its core characteristics of pre- and post-natal growth impairment are shared with all small for gestational age (SGA) children with failure of catch up growth. This includes many children in whom there is as yet no clear mechanism of growth impairment. The aim of this study was to identify novel potential mechanisms of growth impairment in 3-M syndrome, as an exemplar condition for SGA, by examining the transcriptome of skin fibroblast cell lines derived from 3-M patients. Skin fibroblast cell lines have previously been useful in the study of other growth disorders (15, 16). An understanding of the mechanisms of growth impairment in 3-M syndrome could lead to insights into the causation of poor growth in other SGA children and potential targets for molecular diagnostics.

Subjects and methods

Patients

Skin fibroblast cell lines were derived from four 3-M syndrome patients and three control subjects. Biopsies were obtained from the forearm after application of EMLA cream (AstraZeneca). The patients included one male with a homozygous *CUL7* mutation (c.4191delC p.H1379HfsX11), one male with a homozygous *OBSL1* mutation (c.1273insA, p.T425NfsX40, referred to as OBSL1M here), one female with a homozygous *OBSL1* mutation (c.1273insA, p.T425NfsX40, referred to as OBSL1F) and one female with a homozygous *CCDC8* mutation (c.84dup, p.L29X). The three control fibroblast cell lines (two males and one female) were derived from skin obtained during removal of skin tags. All patients and control subjects were prepubertal at the time the skin samples were obtained. All patients with 3-M syndrome had clinical features of the condition including growth impairment.

Cell culture

Fibroblast cells were cultured in 75 cm^2 cell culture flasks (Corning, Tewkesbury, MA, USA) in DMEM (Invitrogen Paisley, Renfrewshire, UK) supplemented to a final concentration with 10% foetal bovine serum (Invitrogen), 50 units/ml penicillin, 50 μg/ml streptomycin, 2 mM glutamine and 2.5 μg/ml amphoteracin B (Invitrogen).

WST-8 cell growth assay

Cells were seeded at a density of 1000 cells/cm^2 in 96-well cell culture plates (Corning) in 100 μl cell culture media: 24 and 72 h after seeding, 10 μl WST-8 was added to each well, the plate was incubated for 2 h at 37 °C before measuring absorbance at 450 nm on a u.v. spectrophotometer (Bio-Rad Benchmark microplate reader, Bio-Rad UK). For each cell line at each time measurement, a minimum of eight independent wells were examined on three separate occasions.

5-Ethynyl-2′-deoxyuridine incorporation

Cells were seeded at a density of 1000 cells/cm^2 into 8-well chamberslides (Scientific Laboratory Supplies, Hessle, Yorkshire, UK) and incubated for 24 h in 600 μl cell culture media at 37 °C in 5% CO_2. After 24 h, the culture medium was removed and replaced with media containing 40 μM 5-ethynyl-2′-deoxyuridine (EdU) for 3 h with the cells incubated in standard conditions. The media was then removed and the cells washed, fixed and permeabilised. EdU incorporation was assessed using the Click-iT EdU Alexa Fluor 488 Imaging Kit *for 50 coverslips (Invitrogen) as per the manufacturer's instructions. DAPI was used to identify the total number of cells present. Three independent fields containing at least 50 cells per field were

http://www.endocrineconnections.org
DOI: 10.1530/EC-13-0065

examined for each cell line and the experiment was repeated on three occasions. A Leica CTR 5000 microscope was used to visualise the cells incorporating EdU.

Cleaved caspase-3 ELISA

Cleaved caspase-3 was measured with the PathScan Cleaved Caspase-3 ELISA (New England Biolabs, Hitchin, Hertfordshire, UK). Cells were seeded in 6-well plates at 1000 cells/cm^2 for each cell line: 48 h after seeding, the media were removed and cell lysate was generated as per the manufacturer's instructions. Absorbance at 450 nm was measured on a u.v. spectrophotometer (Bio-Rad Benchmark microplate reader, Bio-Rad UK).

RNA extraction and transcriptome analysis

RNA was extracted from the fibroblasts using the RNAEasy kit (Qiagen, Manchester, UK) as per the manufacturer's instructions and supplied to the University of Manchester Microarray Facility (Faculty of Life Sciences, University of Manchester, UK). RNA quality was assessed using an Agilent 2100 Bioanalyser: 500 ng of total RNA per cell line was reverse transcribed using a T7 Oligo dT primer. An *in vitro* transcription reaction was used to generate biotinylated cRNA, which was purified, fragmented and hybridised to an Affymetrix HU-133 Plus 2.0 chip (Affymetrix, Santa Clara, CA, USA).

Microarray data were analysed using Propagating Uncertainty Microarray Analysis (PUMA – http://www.bioinf.manchester.ac.uk/resources/puma/). This process obtains a value for expression for each probeset on the microarray chip and involves normalising gene expression both within and between chips. Probesets were defined as being up- or downregulated if there was a $\pm$1.5-fold difference in the expression between the control and 3-M samples with an expression level $>$50 (arbitrary units) in at least one cell line.

PUMA was also used to undertake principle component analysis (PCA) with probability of positive log-ratio (PPLR) to examine any differences in gene expression between control and 3-M fibroblasts. PPLR values closer to $+1$ indicate those probesets that are most likely to be upregulated and values closer to -1 indicate those most likely to be downregulated. In addition to PCA, quality control of the arrays was assessed with dCHIP (http://biosun1.harvard.edu/complab/dchip/).

Gene ontology and pathway analysis were performed with the use of the National Institute's Health Database for Annotation, Visualisation, Integrated Discovery (NIH DAVID) (http://david.abcc.ncifcrf.gov/).

Quantitative PCR

One microgram RNA (derived independently from the samples used for microarray) was reverse transcribed using the high capacity RNA to cDNA kit (Applied Biosystems). *IGF2* and *H19* mRNA levels were assessed using TaqMan assays (Hs01005963_m1 and Hs00262142_g1) with a cyclophyllin A probe (4333763T) for control gene expression. The other genes were assayed using SYBR green with GAPDH as the control gene (primer sequences available on request). Relative fold gene expression for the target gene in the 3-M cell lines was calculated as $2^{-\Delta\Delta CT}$. For each experiment, three independent RNA extractions were assayed with three technical replicates.

Methylation analysis of H19 and IGF2

One microgram peripheral leukocyte or fibroblast-derived genomic DNA was treated with bisulphite using the EZ-DNA Methylation kit, according to manufacturer's instructions (Zymo Research, Orange, CA, USA), except that DNA was eluted in 50 µl. Methylation-specific PCRs were performed in duplicate within the H19 promoter and IGF2 DMR0 (as described in Poole *et al.* (17)) and the products were visualised by capillary electrophoresis on an ABI 3130 Genetic Analyzer (Applied Biosystems). Peak height ratiometry was performed and normalised to control samples.

Pyrosequencing was performed in duplicate, interrogating both the H19 ICR (as described in Poole *et al.* (17)) and IGF2P0 DMR0 (as described in Murrell *et al.* (18)). Primer sequences for all assays are provided in Tables 1 and 2.

Measurement of IGF-II in cell culture medium

Conditioned cell culture medium was obtained by incubating serum-free media with the relevant skin fibroblast cell line for 7 days. IGF-II levels were measured using an Active Non-Extraction IGF-II ELISA (Beckman Coulter, High Wycombe, Buckinghamshire, UK). IGF-II concentrations are much lower in cell culture medium than serum (for which the kit was designed) and this required some amendment to the standard kit protocol. Up to 400 µl conditioned cell culture medium was added to 550 µl sample buffer 1 and incubated at room temperature for 30 min: 950 µl sample buffer 2 was then added and the tube was vortexted. Fifty microlitre of the

http://www.endocrineconnections.org
DOI: 10.1530/EC-13-0065

Table 1 Primer sequences for methylation-specific PCR.

DMR	Chr	Chromosomal location GRCh37	Methylated allele size	Unmethylated allele size	Methylated primer	Unmethylated primer	Universal FAM-labelled primer
H19 promotor	11p15	chr11: 2 019 455–2 019 764	pat 295	mat 305	CGTTTGTTAGTA-GAGTGCGTTCGC-GAGTCG	GGTTGTTTATTGTTT-GTTAGTA-GAGTGTGTTTGTG	ATAACAGAAAAAAC-CCCTTCCTACCAC-CATCAC
IGF2P0	11p15	chr11: 2 169 485–2 169 651	pat 155	mat 163	GTTTGACGAGGT-TAGTGAGG-GACGGCG	ATAGTTTTGTTTGAt-GAGGTTAGT-GAGGGATGGTG	CCAAAACAATTTCCC-TAAAAATACTCATT-CATAC

treated samples were added to each well of the ELISA plate and the remainder of the process was performed as per the manufacturer's instructions. Total protein concentration was measured in the conditioned media using Bio-Rad protein assay dye reagent (Bio-Rad) as per the manufacturer's instructions. Protein concentration of the control media was normalised to 1 and the IGF-II concentration adjusted for the total protein concentration in each cell line's conditioned media.

Results

Whole transcriptome analysis

There were 644 probesets identified as being upregulated and 658 identified as being downregulated in all three groups of 3-M patients compared with controls (Fig. 1). The top 10 up- and downregulated probesets are listed in Tables 3 and 4 respectively. Table 5 lists the top 20 up- and downregulated probesets for each cell line (*CUL7*, *OBSL1* or *CCDC8* mutation) and indicates which of these probesets are shared between more than one group. The majority of probesets is shared between more than one group and this suggests that there is a common set of genes dysregulated in 3-M syndrome.

Among the upregulated probesets were two homeobox genes, *HOXC6*, a transcription factor expressed in the developing skeleton (19), and *HOXA9*, a transcription factor involved in myeloid differentiation linked with increased cell proliferation in leukaemia (20). Other upregulated genes included *GPC6* (loss of function mutations result in the short stature condition omodysplasia (21)) as well as zinc finger protein of cerebellum 1 (*ZIC1*) and *PCP4* both of which are known to be differentially expressed in tumours (22, 23). Three out of the top 10 downregulated probesets represented *IGF2* which encodes a 7.5 kDa secreted hormone known to be a regulator of intra-uterine growth (24).

Q-PCR validation of a six up-and downregulated genes was undertaken (Table 6). In all cases, the Q-PCR result confirmed the findings on the microarray.

Gene ontology analysis of the top 500 up- and downregulated probesets comparing all four 3-M cell lines with controls identified terms including skeletal system morphogenesis, cell adhesion and cell–cell signalling as being over represented (Benjamini–Hochberg adjusted P value <0.05). Cellular compartment terms significantly over-represented all related to the extracellular region.

Of the differentially regulated genes identified, the gene most closely linked with impaired growth was *IGF2*. Hypomethylation of the H19 differentially methylated region leads to *IGF2* silencing in the Silver–Russell syndrome (SRS) (25). SRS shares key features with 3-M

Table 2 Primer sequences for pyrosequencing.

DMR	Chr	Chromosomal location GRCh37	Methylated allele size	Unmethylated allele size	Primer 1	Primer 2 (biotinylated)	Sequencing primer(s)
IGF2 DMR0	11p15	chr11: 2 169 328–2 169 582	NA	NA	TGAGGATGGG-TTTTTGTTTGGTAT	TCCTCAATCCACC-CAAAATAATAT	AAAAGTTATTGGATA-TATAGT or GGGGTGGAGGGT-GTA
H19 ICR1	11p15	chr11: 1 977 650–1 977 877	NA	NA	GTATAGTATATGGG-TATTTTTGGAGG	CCATAAATATCC-TATTCCCAAA-TAACC	GTTTYGGGTTATT-TAAGTT

http://www.endocrineconnections.org
DOI: 10.1530/EC-13-0065

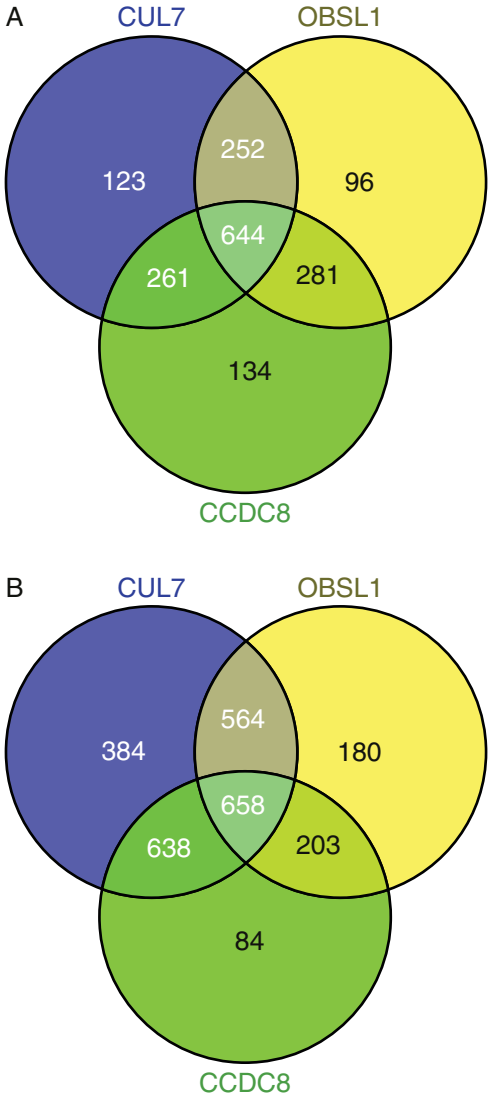

Figure 1
Venn diagrams of (A) up- and (B) downregulated probesets with expression level >50 and fold change (FC) > ±1.5 compared to control.

syndrome, namely the pre- and post-natal growth restriction with normal head size and triangular facies. It was therefore decided to focus further studies on *IGF2*.

IGF2 expression and protein concentrations in conditioned cell culture media

Q-PCR using three independently extracted RNA samples (each sample run in triplicate) confirmed the decrease in *IGF2* expression with relative fold expression of 0.0019±0.0009 for CUL7 ($P<0.001$), 0.0155±0.0021 for OBSL1M ($P<0.001$), 0.0497±0.0170 for OBSL1F ($P<0.001$) and 0.1355±0.0146 for CCDC8 ($P<0.001$) compared with controls (Fig. 2).

Although not present in the top 10 upregulated probesets, the H19 non-coding RNA was represented by the 23rd most upregulated probeset (FC 38, PPLR 1). Q-PCR of H19 confirmed that it was upregulated in all four 3-M cell lines (Fig. 2). Relative fold expression was 2.5±0.8 for CUL7 ($P<0.001$), 140±53 for OBSL1M ($P<0.001$), 72±12 for OBSL1F ($P<0.001$) and 1106±435 for CCDC8 ($P<0.001$).

Concentrations of IGF-II were reduced in conditioned cell culture media from all four 3-M cell lines compared with control cell lines (Fig. 3). The mean IGF-II concentration for the three control cell lines after adjustment for total protein concentration in the media was 10.2±2.9 ng/ml, compared with 0.1±0.2 ng/ml for the CUL7 cell line ($P<0.001$), 0.3±0.4 ng/ml for the OBSL1M cell line ($P<0.001$), 0.4±0.5 ng/ml for the OBSL1F cell line ($P<0.001$) and 1.6±1.3 ng/ml for the CCDC8 cell line ($P<0.001$).

Overexpression of *H19* and silencing of *IGF2* in SRS are caused by changes in methylation in the H19 differentially methylated region. Methylation-specific PCR and pyrosequencing of the *H19* ICR, *H19* promotor and *IGF2* DMR0 identified no differences in methylation between control and 3-M syndrome subjects, for both peripheral leucocyte and fibroblast-derived DNA.

Cell proliferation and apoptosis

Cell proliferation was assessed via incorporation of EdU and by a WST-8 assay. Incorporation of EdU 48 h after its addition to cell culture media was reduced for all 3-M fibroblast cell lines compared with control (Fig. 4A, $P<0.05$), while cell proliferation as measured by colorimetric change induced by WST-8 was reduced at 48 and 72 h after seeding for 3-M fibroblast cell lines compared with control (Fig. 4B, $P<0.05$). Cleaved caspase-3, a biomarker of apoptosis was not significantly different between control and 3-M fibroblasts (Fig. 4C).

Discussion

The aim of this study was to identify novel pathogenic mechanisms underlying the growth failure of patients with 3-M syndrome, which could potentially be relevant to other patients born SGA with the failure of post-natal growth but no defined aetiology. Previous work has examined the role of CUL7 and OBSL1 either in mouse studies or using gene overexpression or knockdown

http://www.endocrineconnections.org
DOI: 10.1530/EC-13-0065

Table 3 Top 10 upregulated probesets comparing all 3-M cell lines ($n=4$) with control ($n=3$).

Gene title	Gene symbol	Mean expression level control	Mean expression level 3-M	Fold difference 3-M/control	PPLR
Zic family member 1	*ZIC1*	0.16	171.85	1087.41	1.00
Purkinje cell protein 4	*PCP4*	0.36	185.70	513.42	1.00
Homeobox C6	*HOXC6*	2.40	615.78	256.07	0.99
Homeobox A10	*HOXA10*	1.40	311.76	223.27	0.55
Homeobox A9	*HOXA9*	1.83	346.95	189.98	1.00
Interleukin 13 receptor, alpha 2	*IL13RA2*	6.27	779.20	124.27	1.00
Collagen, type XIV, alpha 1	*COL14A1*	1.28	145.45	113.88	1.00
Glypican 6	*GPC6*	5.51	591.28	107.25	1.00
Clusterin	*CLU*	7.84	795.86	101.45	1.00
Solute carrier member 15	*SLC6A15*	1.42	117.15	82.29	1.00

PPLR, probability of positive log-ratio.

strategies in immortalised cancer cell lines. The limitations of mouse studies are clear from the death of the mice in the neonatal period (a feature not commonly seen in humans with 3-M syndrome). The mouse thus gives no opportunity to study the effects on post-natal growth and also indicates significant differences in the result of loss of CUL7 between species. Studies using temporary over/under expression strategies in immortalised cells yield useful data, but the extrapolation from these findings to normal human growth is not clear. This study therefore used patient-derived fibroblast cell lines.

It is clear that there is a common set of genes dysregulated in 3-M syndrome. The top upregulated gene was *Zic1*, a transcription factor which, in mouse, is predominantly expressed within the nervous system with the highest levels of expression in the cerebellum (26). *ZIC1* expression is downregulated in gastric carcinomas (23) and increased in desmoid tumour fibroblasts (27) and brain tumours (medulloblastomas and meningiomas) (28, 29). Several other genes in the top 10 upregulated probesets are also overexpressed in tumours including *PCP4* in leiomyomas (22), *HOXC6* in oesophageal (30), breast (31) and lung carcinomas (32) and *IL16RA2* in glioblastomas (33), prostate cancer and adrenocortical tumours (34). This indicates that their overexpression in 3-M fibroblasts could be an attempt to increase cell proliferation. Data on siRNA-mediated knockdown and overexpression of *HOXC6* in a gastric carcinoid cell line are consistent with this hypothesis as overexpression leads to improved growth while loss of *HOXC6* leads to impaired cell growth (35).

Glypican 6 (*GPC6*), in the top 10 downregulated probesets, is a heparan sulphate proteoglycan, which is linked to the extracellular surface of the cell membrane. Glypicans are expressed during development and are thought to control availability of local growth factors (36). Loss of function mutations in GPC6 lead to impaired endochondral ossification and cause the short stature

Table 4 Top 10 downregulated probesets comparing all 3-M cell lines ($n=4$) with control ($n=3$).

Gene title	Gene symbol	Mean expression level control	Mean expression level 3-M	Fold difference 3-M/control	PPLR
Insulin-like growth factor 2	*IGF2*	2118.84	0.06	−38 253.37	0.00
Leptin	*LEP*	64.69	0.10	−642.51	0.00
Insulin-like growth factor 2	*IGF2*	94.15	0.17	−549.78	0.00
Brain expressed, X-linked 1	*BEX1*	369.40	1.30	−283.28	0.00
Prostaglandin D2 synthase 21 kDa (brain)	*PTGDS*	136.49	0.62	−219.06	0.00
Collagen, type IV, alpha 1	*COL4A1*	199.37	1.09	−183.08	0.03
Leucine-rich repeat-containing G protein-coupled receptor 5	*LGR5*	270.20	1.51	−179.24	0.01
Insulin-like growth factor 2	*IGF2*	44.95	0.29	−157.09	0.00
Glutamate receptor, ionotropic, kainate 2	*GRIK2*	44.54	0.35	−126.79	0.00
WAP four-disulfide core domain 1	*WFDC1*	37.84	0.37	−101.50	0.00

PPLR, probability of positive log-ratio.

http://www.endocrineconnections.org
DOI: 10.1530/EC-13-0065

Table 5 Top 20 up- and downregulated probesets in the 3-M group as a whole and in each cell line by mutation.

Up-regulated probesets				Down-regulated probesets			
3-M	CUL7	OBSL1	CCDC8	3-M	CUL7	OBSL1	CCDC8
ZIC1[a]	PCP4[a]	ZIC1[a]	XIST	IGF2[a]	IGF2[a]	IGF2[a]	IGF2[a]
PCP4[a]	ZIC1[a]	PCP4[a]	ZIC1[a]	LEP[a]	LGR5[b]	LEP[a]	CADM1
HOXC6[a]	HOXA10[a]	HOXC6[a]	HOXC6[a]	IGF2[a]	COL4A1[b]	EDIL3[c]	PSG2
HOXA10[a]	COL14A1[b]	COL14A1[b]	HOXA10[a]	–	SFRP2	IGF2[a]	IGF2[a]
HOXA9[a]	HOXA9[a]	SNCA[c]	HOXA9[a]	BEX1[a]	LEP[a]	–	DDX3Y
IL13RA2[a]	IL13RA2[a]	HOXA10[a]	PCP4[a]	PTGDS[b]	DIO2	COL4A1[b]	LGR5
COL14A1[b]	THBS4	HOXA9[a]	PAX6	COL4A1[b]	APOE[c]	BEX1[a]	PTGDS
GPC6[a]	–	CLU[b]	EMCN	LGR5[b]	RARRES2[b]	PTGDS[b]	PSG3
CLU[b]	HOXA11[b]	–	XIST	IGF2[a]	NID2	IGF2[a]	BEX1[a]
SLC6A15[b]	HOXC6[a]	CYP3A5	PAX6	GRIK2[c]	TFAP2A[b]	HAPLN1	RPS4Y1
HOXA10[a]	TNXB	SLC6A15[b]	GPC6[a]	WFDC1[c]	–	IGFBP5	MAOA
HOXA11[b]	KCNB1	IL13RA2[a]	CLU[b]	TFAP2A[b]	LXN	RARRES2[b]	GRIK2
–	WIF1	GPC6[a]	IL13RA2[a]	RARRES2[b]	IGF2[a]	WFDC1[c]	TFAP2A[b]
CLU[b]	GPC6[a]	CLU[b]	HOXA10[a]	APOE[c]	TLR4[a]	HAPLN1	LEP[a]
–	HOXA10[a]	SPON1[c]	XIST	WNT5A[c]	APOE[c]	SYNPO2[c]	IGF2[a]
ABCA6[b]	ST8SIA1	SCARA3[c]	WISP1	EDIL3[c]	ITIH5[c]	WNT5A[c]	TRPC6
SCARA3[c]	ACE	HOXA10[a]	THBD	SIM2	PMEPA1	IGFBP7	FAM19A5
HOXA9[a]	SLC6A15[b]	ABCA6[b]	THBD	–	PSG7	TPD52L1	ITIH5[c]
SPON1[c]	COL14A1[b]	SPON1[c]	H19	SYNPO2[c]	DIO2	MRVI1	ITIH5[c]
TBX5	ABCA6[b]	SNX10	SNCA[c]	PPP1R14A	BEX1[a]	STXBP6	USP9Y

[a]Probesets present in all groups; [b]probesets present in the 3-M group and two mutation groups; [c]probesets present in the 3-M group and one mutation group. –, probeset is designed to a gene which was not named at the time of the study.

condition omodysplasia (21). Loss of function mutations in glypican 3 (GPC3) causes the overgrowth disorder Simpson–Golabi–Behmel syndrome (SGBS). GPC3 interacts with IGF-II and it was initially hypothesised that GPC3 binds to and sequesters IGF-II; thus the overgrowth in SGBS is caused by increased availability of IGF-II (37). More recent data on mouse indicate that the overgrowth of *Gpc3* null mice is independent of IGF-II (38), while data on the role of GPC3 in the growth of cancer cell lines are inconsistent with some studies suggesting that GPC3 suppressed growth in an IGF-dependant manner (39) while others identified GPC3 as a growth-promoting protein (40, 41). Of note, of the two probesets in our microarray designed to detect the expression of GPC3, one did not detect expression of GPC3 (defined in this study as an expression level >50) in any cell line while the other probeset identified a modest downregulation (FC −1.76 PPLR 0.44).

Three of the top 10 downregulated probesets represented *IGF2* with the smallest fold change being −157. The second most downregulated probeset represented leptin, a 16 kDa adipocyte-derived hormone which plays a central role in the regulation of body weight, both by inhibiting food intake and increasing energy expenditure (42, 43). Downregulation of leptin in 3-M syndrome may represent a response to the patients slim body habitus or be a signal to drive energy intake in order to promote growth. *BEX1*, *PTGDS*,

Table 6 Additional validation of gene expression data. Expression of genes identified as being up- or downregulated in the microarray were assessed with Q-PCR. Relative fold expression for each of the seven genes analysed is given for each of the four 3-M cell lines. Expression was normalised to GAPDH and mean control cell line expression.

	CUL7		OBSL1 F		OBSL1 M		CCDC8	
Gene	Relative expression	*P*	Relative expression	*P*	Relative expression	*P*	Relative expression	*P*
BEX1	0.06±0.01	<0.001	0.15±0.20	<0.001	0.03±0.02	<0.001	0.20±0.24	<0.001
LEP	0.07±0.04	<0.001	0.06±0.03	<0.001	0.01±0.00	<0.001	0.04±0.01	<0.001
ZIC1	946±462	<0.001	496±186	0.004	1200±891	<0.001	759±498	0.002
HOXC6	31±24	0.006	88±55	0.001	51±38	0.005	100±87	0.009
HOXA9	690±586	0.008	501±466	0.012	349±296	0.008	399±342	0.008
GPC6	35±6	<0.001	44±10	<0.001	7±2	<0.001	5±1	<0.001

http://www.endocrineconnections.org
DOI: 10.1530/EC-13-0065

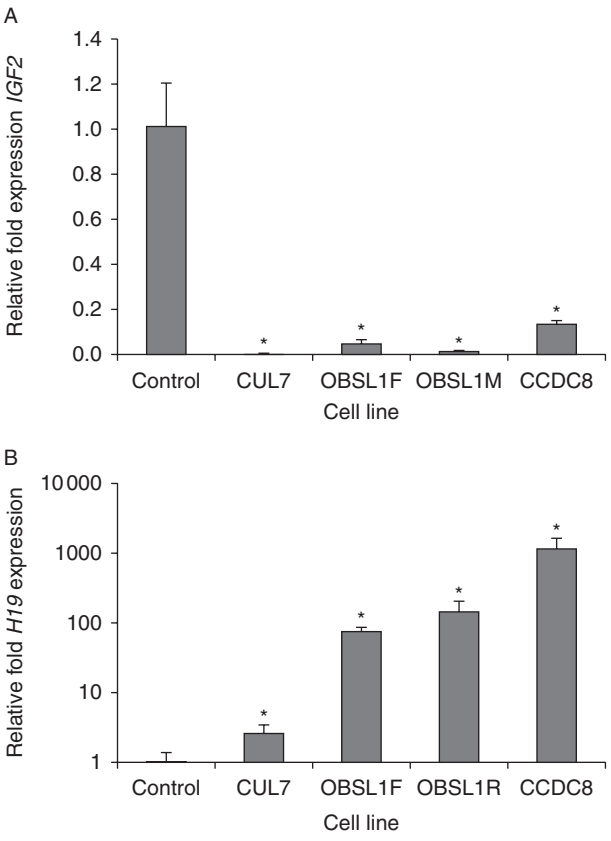

Figure 2
Relative fold expression of (A) *IGF2* and (B) *H19* measured using quantitative PCR in all 3-M cell lines. Expression of *IGF2* is reduced while *H19* is increased. *$P<0.05$.

GRIK2 and *WFDC1*, also in the top 10 downregulated probesets, have all been identified as downregulated in tumours (44, 45) or as inhibitors of cell proliferation in immortalised cell lines (46, 47, 48). Thus in common with several of the genes identified as being upregulated these changes are likely to represent a response to increase cell proliferation.

While many of the identified changes in gene expression, such as the overexpression of GPC6, are likely to be a compensatory response to the growth impairment, we hypothesised that there would be a smaller number of genes with altered expression which are key to the pathogenic process underlying 3-M syndrome. The most obvious of such candidate was *IGF2*, which was represented by three of the top 10 downregulated probesets. The encoded protein IGF-II is a 7.5 kDa secreted hormone that acts to increase cell proliferation via stimulation of the IGF1R. It is widely expressed during the development and is a major regulator of intra-uterine growth. *IGF2* expression is regulated by methylation of the H19 region (H19 DMR); hypomethylation of the H19 DMR with subsequent *IGF2* gene silencing leads to the short stature condition SRS (25). SRS shares several key features with 3-M syndrome: intra-uterine growth retardation, post-natal growth impairment, relatively normal head size, normal intelligence and a triangular shaped face. Other downregulated genes identified which could potentially be implicated in the pathogenesis of 3-M syndrome included *LGR5* (a member of the G-protein-coupled receptor superfamily) and *COL4A1* (the main component of type IV collagen which forms basement membrane); silencing of expression of these genes is associated with decreased cell proliferation (49) while in tumours (50, 51), they have been found to be upregulated. Of the top 10 upregulated probesets, the only gene identified as potentially being involved in the pathogenesis of 3-M syndrome was COL14A1, a large glycoprotein of the extracellular matrix which has an anti-proliferative effect on fibroblasts (52) and knockdown in renal cancer cells, which results in increased growth (53).

Given the findings of reduced IGF-II production from 3-M syndrome fibroblasts, it is likely that local production of IGF-II is reduced with loss of its autocrine/paracrine effects. Loss of local IGF-II in the growth plates and other tissues leads to growth impairment both pre- and post-natally. The reduced cell proliferation with no change found in a biomarker of apoptosis would be consistent with a reduction in the presence of a growth factor. While there is significant phenotypic overlap between 3-M

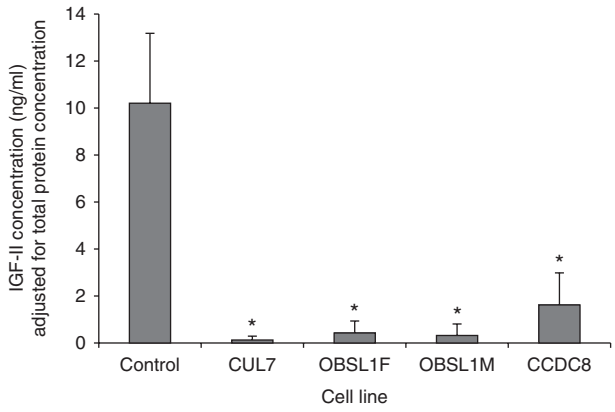

Figure 3
IGF-II concentrations in conditioned cell culture media are significantly reduced for all 3-M syndrome fibroblast cell lines. *$P<0.05$ compared to control. IGF-II concentrations are adjusted for total protein concentration in the cell culture media.

http://www.endocrineconnections.org
DOI: 10.1530/EC-13-0065

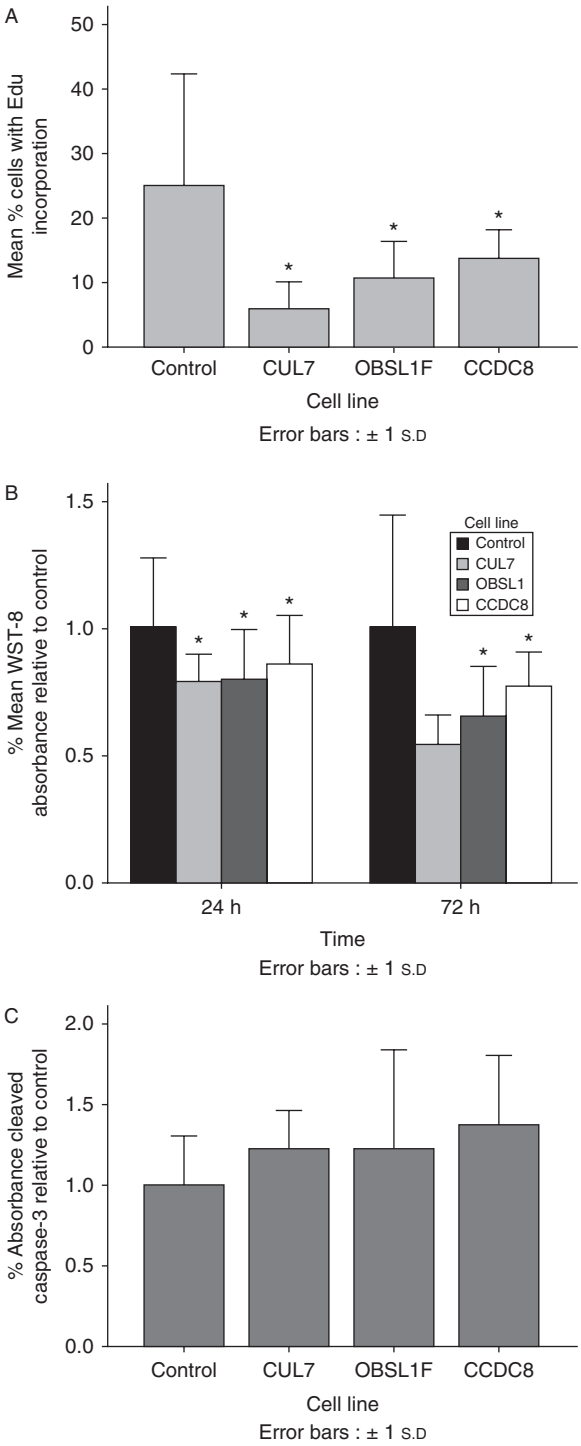

Figure 4
Reduced cell proliferation with no increase in apoptosis is seen in fibroblasts from 3-M syndrome patients. (A) Decreased incorporation of EdU measured at 48 h. (B) Decreased cell proliferation at 24 and 72 h after seeding measured by WST-8. (C) No difference in apoptosis as measured by Cleaved Caspase-3 ELISA. *$P<0.05$.

syndrome and SRS, there are also phenotypic differences. These are likely to be due to additional functions of the proteins affected in 3-M syndrome.

The mechanisms through which *IGF2* expression is reduced in 3-M syndrome remain unclear. It does not appear to be via the same mechanism as is found in SRS, i.e. hypomethylation at H19 DMR. It is possible that there may be an epigenetic change which has not been recognised but this appears unlikely. There may be another mechanism, such as alteration in CCCTC-binding factor concentrations or activity that could lead to the same gene expression pattern.

Height at presentation in 3-M syndrome is lowest in patients with *CUL7* mutations and highest in those with *CCDC8* mutations (13). Of interest, the pattern of *IGF2* expression and IGF-II production mirrored the growth phenotype of the patients with the lowest IGF-II production in the CUL7 cell line and the highest IGF-II production in the CCDC8 cell line.

In conclusion, this study demonstrates that there is reduced expression of *IGF2* in 3-M syndrome linking the pathogenesis to that of SRS. The mechanisms underlying the silencing of *IGF2* in 3-M syndrome are unclear, but do not appear to involve hypomethylation at the H19 DMR.

Declaration of interest
The authors declare that there is no conflict of interest that could be perceived as prejudicing the impartiality of the research reported.

Funding
P G Murray was a MRC Clinical Training Fellow. The support of the Manchester NIHR Biomedical Research Centre is acknowledged.

References

1 Huber C, Dias-Santagata D, Glaser A, O'Sullivan J, Brauner R, Wu K, Xu X, Pearce K, Wang R, Uzielli ML *et al*. Identification of mutations in CUL7 in 3-M syndrome. *Nature Genetics* 2005 **37** 1119–1124. (doi:10.1038/ng1628)
2 Hanson D, Murray PG, Sud A, Temtamy SA, Aglan M, Superti-Furga A, Holder SE, Urquhart J, Hilton E, Manson FD *et al*. The primordial growth disorder 3-M syndrome connects ubiquitination to the cytoskeletal adaptor OBSL1. *American Journal of Human Genetics* 2009 **84** 801–806. (doi:10.1016/j.ajhg.2009.04.021)
3 Hanson D, Murray PG, O'Sullivan J, Urquhart J, Daly S, Bhaskar SS, Biesecker LG, Skae M, Smith C, Cole T *et al*. Exome sequencing identifies CCDC8 mutations in 3-M syndrome, suggesting that CCDC8 contributes in a pathway with CUL7 and OBSL1 to control human growth. *American Journal of Human Genetics* 2011 **89** 148–153. (doi:10.1016/j.ajhg.2011.05.028)
4 Dias DC, Dolios G, Wang R & Pan ZQ. CUL7: a DOC domain-containing cullin selectively binds Skp1.Fbx29 to form an SCF-like complex. *PNAS* 2002 **99** 16601–16606. (doi:10.1073/pnas.252646399)

http://www.endocrineconnections.org
DOI: 10.1530/EC-13-0065

5 Geisler SB, Robinson D, Hauringa M, Raeker MO, Borisov AB, Westfall MV & Russell MW. Obscurin-like 1, OBSL1, is a novel cytoskeletal protein related to obscurin. *Genomics* 2007 **89** 521–531. (doi:10.1016/j.ygeno.2006.12.004)

6 Clayton PE, Hanson D, Magee L, Murray PG, Saunders E, Abu-Amero SN, Moore GE & Black GC. Exploring the spectrum of 3-M syndrome, a primordial short stature disorder of disrupted ubiquitination. *Clinical Endocrinology* 2012 **77** 335–342. (doi:10.1111/j.1365-2265.2012.04428.x)

7 Arai T, Kasper JS, Skaar JR, Ali SH, Takahashi C & DeCaprio JA. Targeted disruption of p185/Cul7 gene results in abnormal vascular morphogenesis. *PNAS* 2003 **100** 9855–9860. (doi:10.1073/pnas.1733908100)

8 Okabe H, Lee SH, Phuchareon J, Albertson DG, McCormick F & Tetsu O. A critical role for FBXW8 and MAPK in cyclin D1 degradation and cancer cell proliferation. *PLoS ONE* 2006 **1** e128. (doi:10.1371/journal.pone.0000128)

9 Xu X, Sarikas A, Dias-Santagata DC, Dolios G, Lafontant PJ, Tsai SC, Zhu W, Nakajima H, Nakajima HO, Field LJ *et al*. The CUL7 E3 ubiquitin ligase targets insulin receptor substrate 1 for ubiquitin-dependent degradation. *Molecular Cell* 2008 **30** 403–414. (doi:10.1016/j.molcel.2008.03.009)

10 Andrews P, He YJ & Xiong Y. Cytoplasmic localized ubiquitin ligase cullin 7 binds to p53 and promotes cell growth by antagonizing p53 function. *Oncogene* 2006 **25** 4534–4548. (doi:10.1038/sj.onc.1209490)

11 Kim SS, Shago M, Kaustov L, Boutros PC, Clendening JW, Sheng Y, Trentin GA, Barsyte-Lovejoy D, Mao DY, Kay R *et al*. CUL7 is a novel antiapoptotic oncogene. *Cancer Research* 2007 **67** 9616–9622. (doi:10.1158/0008-5472.CAN-07-0644)

12 Jung P, Verdoodt B, Bailey A, Yates JR III, Menssen A & Hermeking H. Induction of cullin 7 by DNA damage attenuates p53 function. *PNAS* 2007 **104** 11388–11393. (doi:10.1073/pnas.0609467104)

13 Hanson D, Murray PG, Coulson T, Sud A, Omokanye A, Stratta E, Sakhinia F, Bonshek C, Wilson LC, Wakeling E *et al*. Mutations in CUL7, OBSL1 and CCDC8 in 3-M syndrome lead to disordered growth factor signalling. *Journal of Molecular Endocrinology* 2012 **49** 267–275. (doi:10.1530/JME-12-0034)

14 Huber C, Fradin M, Edouard T, Le Merrer M, Alanay Y, Da Silva DB, David A, Hamamy H, van Hest L, Lund AM *et al*. OBSL1 mutations in 3-M syndrome are associated with a modulation of IGFBP2 and IGFBP5 expression levels. *Human Mutation* 2009 **31** 20–26. (doi:10.1002/humu.21150)

15 Freeth JS, Ayling RM, Whatmore AJ, Towner P, Price DA, Norman MR & Clayton PE. Human skin fibroblasts as a model of growth hormone (GH) action in GH receptor-positive Laron's syndrome. *Endocrinology* 1997 **138** 55–61. (doi:10.1210/en.138.1.55)

16 Westwood M, Tajbakhsh SH, Siddals KW, Whatmore AJ & Clayton PE. Reduced pericellular sensitivity to IGF-I in fibroblasts from girls with Turner syndrome: a mechanism to impair clinical responses to GH. *Pediatric Research* 2011 **70** 25–30. (doi:10.1203/PDR.0b013e31821b570b)

17 Poole RL, Baple E, Crolla JA, Temple IK & Mackay DJ. Investigation of 90 patients referred for molecular cytogenetic analysis using aCGH uncovers previously unsuspected anomalies of imprinting. *American Journal of Medical Genetics. Part A* 2010 **152A** 1990–1993. (doi:10.1002/ajmg.a.33530)

18 Murrell A, Ito Y, Verde G, Huddleston J, Woodfine K, Silengo MC, Spreafico F, Perotti D, De Crescenzo A & Sparago A. Distinct methylation changes at the IGF2-H19 locus in congenital growth disorders and cancer. *PLoS ONE* 2008 **3** e1849. (doi:10.1371/journal.pone.0001849)

19 Sharpe PT, Miller JR, Evans EP, Burtenshaw MD & Gaunt SJ. Isolation and expression of a new mouse homeobox gene. *Development* 1988 **102** 397–407.

20 Whelan JT, Ludwig DL & Bertrand FE. HoxA9 induces insulin-like growth factor-1 receptor expression in B-lineage acute lymphoblastic leukemia. *Leukemia* 2008 **22** 1161–1169. (doi:10.1038/leu.2008.57)

21 Campos-Xavier AB, Martinet D, Bateman J, Belluoccio D, Rowley L, Tan TY, Baxová A, Gustavson KH, Borochowitz ZU, Innes AM *et al*. Mutations in the heparan-sulfate proteoglycan glypican 6 (GPC6) impair endochondral ossification and cause recessive omodysplasia. *American Journal of Human Genetics* 2009 **84** 760–770. (doi:10.1016/j.ajhg.2009.05.002)

22 Kanamori T, Takakura K, Mandai M, Kariya M, Fukuhara K, Kusakari T, Momma C, Shime H, Yagi H, Konishi M *et al*. PEP-19 overexpression in human uterine leiomyoma. *Molecular Human Reproduction* 2003 **9** 709–717. (doi:10.1093/molehr/gag088)

23 Wang LJ, Jin HC, Wang X, Lam EKY, Zhang JB, Liu X, Chan FKL, Si JM & Sung JJY. ZIC1 is downregulated through promoter hypermethylation in gastric cancer. *Biochemical and Biophysical Research Communications* 2009 **379** 959–963. (doi:10.1016/j.bbrc.2008.12.180)

24 Baker J, Liu JP, Robertson EJ & Efstratiadis A. Role of insulin-like growth factors in embryonic and postnatal growth. *Cell* 1993 **75** 73–82.

25 Gicquel C, Rossignol S, Cabrol S, Houang M, Steunou V, Barbu V, Danton F, Thibaud N, Le Merrer M, Burglen L *et al*. Epimutation of the telomeric imprinting center region on chromosome 11p15 in Silver–Russell syndrome. *Nature Genetics* 2005 **37** 1003–1007. (doi:10.1038/ng1629)

26 Aruga J, Yokota N, Hashimoto M, Furuichi T, Fukuda M & Mikoshiba K. A novel zinc finger protein, zic, is involved in neurogenesis, especially in the cell lineage of cerebellar granule cells. *Journal of Neurochemistry* 1994 **63** 1880–1890. (doi:10.1046/j.1471-4159.1994.63051880.x)

27 Pourebrahim R, Van Dam K, Bauters M, De Wever I, Sciot R, Cassiman JJ & Tejpar S. ZIC1 gene expression is controlled by DNA and histone methylation in mesenchymal proliferations. *FEBS Letters* 2007 **581** 5122–5126. (doi:10.1016/j.febslet.2007.09.061)

28 Aruga J, Nozaki Y, Hatayama M, Odaka YS & Yokota N. Expression of ZIC family genes in meningiomas and other brain tumors. *BMC Cancer* 2010 **10** 79. (doi:10.1186/1471-2407-10-79)

29 Yokota N, Aruga J, Takai S, Yamada K, Hamazaki M, Iwase T, Sugimura H & Mikoshiba K. Predominant expression of human zic in cerebellar granule cell lineage and medulloblastoma. *Cancer Research* 1996 **56** 377–383.

30 Chen KN, Gu ZD, Ke Y, Li JY, Shi XT & Xu GW. Expression of 11 HOX genes is deregulated in esophageal squamous cell carcinoma. *Clinical Cancer Research* 2005 **11** 1044–1049.

31 Bodey B, Bodey B Jr, Siegel SE & Kaiser HE. Immunocytochemical detection of the homeobox B3, B4, and C6 gene products in breast carcinomas. *Anticancer Research* 2000 **20** 3281–3286.

32 Bodey B, Bodey B Jr, Groger AM, Siegel SE & Kaiser HE. Immunocytochemical detection of homeobox B3, B4, and C6 gene product expression in lung carcinomas. *Anticancer Research* 2000 **20** 2711–2716.

33 Marie SK, Okamoto OK, Uno M, Hasegawa AP, Oba-Shinjo SM, Cohen T, Camargo AA, Kosoy A, Carlotti CG Jr, Toledo S *et al*. Maternal embryonic leucine zipper kinase transcript abundance correlates with malignancy grade in human astrocytomas. *International Journal of Cancer* 2008 **122** 807–815. (doi:10.1002/ijc.23189)

34 Fernandez-Ranvier GG, Weng J, Yeh RF, Khanafshar E, Suh I, Barker C, Duh QY, Clark OH & Kebebew E. Identification of biomarkers of adrenocortical carcinoma using genomewide gene expression profiling. *Archives of Surgery* 2008 **143** 841–846 discussion 6. (doi:10.1001/archsurg.143.9.841)

35 Fujiki K, Duerr EM, Kikuchi H, Ng A, Xavier RJ, Mizukami Y, Imamura T, Kulke MH & Chung DC. Hoxc6 is overexpressed in gastrointestinal carcinoids and interacts with JunD to regulate tumor growth. *Gastroenterology* 2008 **135** 907–16, 916.e1–2. (doi:10.1053/j.gastro.2008.06.034)

36 Filmus J. Glypicans in growth control and cancer. *Glycobiology* 2001 **11** 19R–23R. (doi:10.1093/glycob/11.3.19R)

37 Pilia G, Hughes-Benzie RM, MacKenzie A, Baybayan P, Chen EY, Huber R, Neri G, Cao A, Forabosco A & Schlessinger D. Mutations in GPC3, a glypican gene, cause the Simpson–Golabi–Behmel overgrowth syndrome. *Nature Genetics* 1996 **12** 241–247. (doi:10.1038/ng0396-241)

http://www.endocrineconnections.org
DOI: 10.1530/EC-13-0065

38 Chiao E, Fisher P, Crisponi L, Deiana M, Dragatsis I, Schlessinger D, Pilia G & Efstratiadis A. Overgrowth of a mouse model of the Simpson–Golabi–Behmel syndrome is independent of IGF signaling. *Developmental Biology* 2002 **243** 185–206. (doi:10.1006/dbio.2001.0554)
39 Sakurai M, Shibata K, Umezu T, Kajiyama H, Yamamoto E, Ino K, Nawa A & Kikkawa F. Growth-suppressing function of glypican-3 (GPC3) via insulin like growth factor II (IGF-II) signaling pathway in ovarian clear cell carcinoma cells. *Gynecologic Oncology* 2010 **119** 332–336. (doi:10.1016/j.ygyno.2010.07.013)
40 Cheng W, Tseng CJ, Lin TT, Cheng I, Pan HW, Hsu HC & Lee YM. Glypican-3-mediated oncogenesis involves the insulin-like growth factor-signaling pathway. *Carcinogenesis* 2008 **29** 1319–1326. (doi:10.1093/carcin/bgn091)
41 Sun CK, Chua MS, He J & So SK. Suppression of glypican 3 inhibits growth of hepatocellular carcinoma cells through up-regulation of TGF-β2. *Neoplasia* 2011 **13** 735–747. (doi:10.1593/neo.11664)
42 Montague CT, Farooqi IS, Whitehead JP, Soos MA, Rau H, Wareham NJ, Sewter CP, Digby JE, Mohammed SN, Hurst JA *et al*. Congenital leptin deficiency is associated with severe early-onset obesity in humans. *Nature* 1997 **387** 903–908. (doi:10.1038/43185)
43 Zhang Y, Proenca R, Maffei M, Barone M, Leopold L & Friedman JM. Positional cloning of the mouse obese gene and its human homologue. *Nature* 1994 **372** 425–432. (doi:10.1038/372425a0)
44 Arslan AA, Gold LI, Mittal K, Suen TC, Belitskaya-Levy I, Tang MS & Toniolo P. Gene expression studies provide clues to the pathogenesis of uterine leiomyoma: new evidence and a systematic review. *Human Reproduction* 2005 **20** 852–863. (doi:10.1093/humrep/deh698)
45 Wu CS, Lu YJ, Li HP, Hsueh C, Lu CY, Leu YW, Liu HP, Lin KH, Hui-Ming Huang T & Chang YS. Glutamate receptor, ionotropic, kainate 2 silencing by DNA hypermethylation possesses tumor suppressor function in gastric cancer. *International Journal of Cancer* 2010 **126** 2542–2552. (doi:10.1002/ijc.24958)
46 Vilar M, Murillo-Carretero M, Mira H, Magnusson K, Besset V & Ibanez CF. Bex1, a novel interactor of the p75 neurotrophin receptor, links neurotrophin signaling to the cell cycle. *EMBO Journal* 2006 **25** 1219–1230. (doi:10.1038/sj.emboj.7601017)
47 Larsen M, Ressler SJ, Gerdes MJ, Lu B, Byron M, Lawrence JB & Rowley DR. The WFDC1 gene encoding ps20 localizes to 16q24, a region of LOH in multiple cancers. *Mammalian Genome* 2000 **11** 767–773. (doi:10.1007/s003350010135)
48 Madar S, Brosh R, Buganim Y, Ezra O, Goldstein I, Solomon H, Kogan I, Goldfinger N, Klocker H & Rotter V. Modulated expression of WFDC1 during carcinogenesis and cellular senescence. *Carcinogenesis* 2009 **30** 20–27. (doi:10.1093/carcin/bgn232)
49 Tanese K, Fukuma M, Yamada T, Mori T, Yoshikawa T, Watanabe W, Ishiko A, Amagai M, Nishikawa T & Sakamoto M. G-protein-coupled receptor GPR49 is upregulated in basal cell carcinoma and promotes cell proliferation and tumor formation. *American Journal of Pathology* 2008 **173** 835–843. (doi:10.2353/ajpath.2008.071091)
50 Chen C, Méndez E, Houck J, Fan W, Lohavanichbutr P, Doody D, Yueh B, Futran ND, Upton M, Farwell DG *et al*. Gene expression profiling identifies genes predictive of oral squamous cell carcinoma. *Cancer Epidemiology, Biomarkers & Prevention* 2008 **17** 2152–2162. (doi:10.1158/1055-9965.EPI-07-2893)
51 Liu Y, Carson-Walter EB, Cooper A, Winans BN, Johnson MD & Walter KA. Vascular gene expression patterns are conserved in primary and metastatic brain tumors. *Journal of Neuro-Oncology* 2010 **99** 13–24. (doi:10.1007/s11060-009-0105-0)
52 Ruehl M, Erben U, Schuppan D, Wagner C, Zeller A, Freise C, Al-Hasani H, Loesekann M, Notter M, Wittig BM *et al*. The elongated first fibronectin type III domain of collagen XIV is an inducer of quiescence and differentiation in fibroblasts and preadipocytes. *Journal of Biological Chemistry* 2005 **280** 38537–38543. (doi:10.1074/jbc.M502210200)
53 Morris MR, Ricketts C, Gentle D, Abdulrahman M, Clarke N, Brown M, Kishida T, Yao M, Latif F & Maher ER. Identification of candidate tumour suppressor genes frequently methylated in renal cell carcinoma. *Oncogene* 2010 **29** 2104–2117. (doi:10.1038/onc.2009.493)

Received in final form 17 September 2013
Accepted 22 October 2013